



An ISPH model for flow-like landslides and interaction with structures ^{*}

Dongfang Liang (梁东方)^{1,2}, Xuzhen He³, Jing-xin Zhang (张景新)^{1,2}

1. State Key Laboratory of Ocean Engineering, Shanghai Jiao Tong University, Shanghai 200240, China,
E-mail: d.liang@sjtu.edu.cn

2. Collaborative Innovation Center for Advanced Ship and Deep-Sea Exploration, Shanghai 200240, China

3. Institut für Geotechnik, Universität für Bodenkultur Wien, Feistmantelstrasse 4, 1180 Wien, Austria

(Received April 16, 2017, Revised July 7, 2017)

Abstract: An incompressible smoothed particle hydrodynamics (ISPH) model has been developed to investigate the flow-like landslide phenomena. The landslide mass is idealized as rigid and perfectly-plastic material with a constant density. Unlike the widely-used explicit smoothed particle hydrodynamics (SPH) models for landslides, the Chorin's projection method is used herein to implicitly solve the normal stress via a pressure Poisson equation, leading to a realistic distribution of instantaneous stress fields free of spurious fluctuations. The capability of the model is demonstrated through three case studies, including the idealized granular flow, landslide interaction with a rigid barrier, and a historical cut-slope landslide in Hong Kong.

Key words: Landslides, smoothed particle hydrodynamics, granular flows, meshfree methods

Landslides involve the rapid downslope movement of soil mass under gravity. The widely-used mesh-based methods suffer from grid distortion, which leads to computational inaccuracy and numerical instability. As an alternative, the meshfree methods can easily cope with the large soil deformation. The smoothed particle hydrodynamics (SPH) method is probably the oldest meshfree method, which represents the continuum with a number of discrete particles^[1-3]. Apart from avoiding the mesh tangling problem, the SPH method also has other attractive characteristics. It can significantly reduce computational costs, as discretization is only needed where the landslide mass is present rather than over the entire run-out space. The SPH method can easily track the history-dependent variables, as unknowns are defined on the moving particles.

Almost all the previous SPH models in soil mechanics employ explicit SPH schemes in a similar way to the weakly-compressible SPH models in computational fluid dynamics (CFD). Without complicated

numerical treatments, such as pressure filter, viscous damping and stress regularization, they generate spurious stress oscillations, despite the accurately-predicted velocity field and thus continuum deformation. These nonphysical oscillations pose difficulties to the deployment of sophisticated constitutive models. The present study adopts an implicit SPH method, which has been proved to produce smooth stress field in CFD.

The motion of an incompressible continuum can be modelled by the governing equations below:

$$\frac{\partial v_i}{\partial x_i} = 0 \quad (1)$$

$$\frac{dv_i}{dt} = -\frac{1}{\rho} \frac{\partial p}{\partial x_i} - \frac{1}{\rho} \frac{\partial s_{ij}}{\partial x_j} + g_i \quad (2)$$

where t and x_i are time and spatial coordinate respectively, ρ is density, v_i is velocity, p is normal stress, s_{ij} is deviatoric stress tensor, g_i is gravitational acceleration. Here, we adopt the convention that compression is positive. Because soil in flow-like landslides should have undergone large deformations, it is expected to stay in the critical state. Hence, we ignore the stress ratio variation and

^{*} Project supported by the National Natural Science Foundation of China (Grant No. 51479111), the Ministry of Education and State Administration of Foreign Experts Affairs 111 Project (Grant No. B17015).

Biography: Dongfang Liang (1975-), Male, Professor

dilatancy. Therefore, soil is modelled as an incompressible and rigid-perfectly plastic material with a Coulomb yield surface. With the coaxial assumption, the following relationship holds

$$s_{ij} = p \sin \phi_{\text{crit}} \frac{\dot{\epsilon}_{ij}}{|\dot{\epsilon}_{ij}|} \quad (3)$$

where ϕ_{crit} is the internal friction angle, $\dot{\epsilon}_{ij}$ is the deviatoric strain rate tensor. This relationship is often referred to as the Drucker-Prager yield criterion. The strain rate tensor and its deviatoric counterpart are:

$$\dot{\epsilon}_{ij} = -\frac{1}{2} \left(\frac{\partial v_i}{\partial x_j} + \frac{\partial v_j}{\partial x_i} \right) \quad (4)$$

$$\dot{\epsilon}_{ij} = \dot{\epsilon}_{ij} - \frac{\dot{\epsilon}_{kk}}{3} \delta_{ij} \quad (5)$$

where δ_{ij} is Kronecker delta. The projection method is used to solve the above equations by decoupling the velocity and normal stress calculations. This projection method was first implemented in CFD. It first considers only the gravity and deviatoric stress terms in the momentum equation to obtain an intermediate velocity field, which is subsequently modified to satisfy the incompressible condition. The intermediate and final velocities are:

$$\frac{v_i^{n*} - v_i^n}{\Delta t} = -\frac{1}{\rho^n} \frac{\partial s_{ij}^n}{\partial x_j} + g_i \quad (6)$$

$$\frac{v_i^{n+1} - v_i^{n*}}{\Delta t} = -\frac{1}{\rho^n} \frac{\partial p^{n+1}}{\partial x_i} \quad (7)$$

where Δt is the time step, the subscripts n , n^* and $n+1$ denote time levels. To guarantee incompressibility, the following Poisson equation is solved to update the normal stress, p^{n+1}

$$\frac{\partial}{\partial x_i} \left(\frac{1}{\rho^n} \frac{\partial p^{n+1}}{\partial x_i} \right) = \frac{1}{\Delta t} \frac{\partial v_i^{n*}}{\partial x_i} = \frac{\rho^n - \rho^{n*}}{\rho^n \Delta t^2} \quad (8)$$

Finally, the particle's new position is updated according to the flow velocity.

Using the SPH approximation, each term in the partial differential Eqs.(6)-(8) can be expressed with the kernel function W and its spatial derivatives $\partial W / \partial x_i$. In summary, the SPH discretization of the above equations gives:

$$\frac{v_i^{a,n*} - v_i^{a,n}}{\Delta t} = -\sum_{b=1}^{N_{ei}} m^b \left[\frac{s_{ij}^{a,n}}{(\rho^{a,n})^2} + \frac{s_{ij}^{b,n}}{(\rho^{b,n})^2} \right] \frac{\partial W^{ab,n}}{\partial x_j^a} + g_i \quad (9)$$

$$\sum_{b=1}^{N_{ei}} m^b \frac{8}{(\rho^{a,n} + \rho^{b,n})^2} \frac{x_i^{ab,n} \nabla_i W^{ab,n}}{(r^{ab,n})^2 + \eta^2} (p^{a,n+1} - p^{b,n+1}) = \frac{1}{\rho^{a,n} \Delta t^2} (\rho^{a,n} - \sum_{b=1}^{N_{ei}} m^b m^b W^{ab,n*}) \quad (10)$$

$$\frac{v_i^{a,n+1} - v_i^{a,n*}}{\Delta t} = -\sum_{b=1}^{N_{ei}} m^b \left[\frac{p^{a,n+1}}{(\rho^{a,n})^2} + \frac{p^{b,n+1}}{(\rho^{b,n})^2} \right] \frac{\partial W^{ab,n}}{\partial x_i^a} \quad (11)$$

where the superscript a represents the particle in consideration, b is the index of a neighbouring particle of a , N_{ei} is the total number of neighbours in the support domain of particle a , m is the mass of a particle, r^{ab} is the distance between particles a and b , W^{ab} is the value of the kernel function between a and b , η is a small value to prevent numerical instability when particles get very close.

In the landslide analysis, there are generally two types of boundaries: the free surface and the solid surface. The free surface boundary condition is implemented by first finding the free surface particles and then equating all stresses to zero. Wall particles and dummy particles are used to facilitate prescribing the solid boundary condition. The non-penetration condition is enforced at solid surfaces and the tangential drag force is equated to the normal reaction multiplied by the wall frictional coefficient. Detailed numerical treatments include the renormalized kernel and its gradient in the case of particle deficiency.

The first case study simulates the granular flow along a slope. The corresponding experiment used 50 liters of quartz sand, with an angle of repose (AOR) of 33° [4]. The slope angle was 50° and the drop height was 1.414 m. The sand was initially piled behind a gate perpendicular to the slope, which was suddenly lifted with an opening of 60 mm. Corresponding to the small opening, a thin layer of sand is observed on the slope, as shown in Figs.1(a), 1(b). The initial particle spacing is 4 mm, resulting in a total of 9 736 particles. The final deposition profile observed in the experiment is indicated with a thin solid line, which shows a slope angle in the middle section to be equal to the AOR. Figure 1(a) shows the moment when some soil has been deposited at the toe. The present model can satisfactorily reproduce the flow onto the horizontal plane, with a correct shape of the final deposition.

This example also highlights some discrepancies in the cross-sectional area, which reveal the limitations of the present model. The incompressible model cannot reproduce the volume change of the collapsed material. In reality, granular materials may contract or dilate, depending on its initial state, to a critical state void ratio during mobilization. The experimental result in Fig.1 shows around 10% increase in the final cross-sectional area of the deposition.

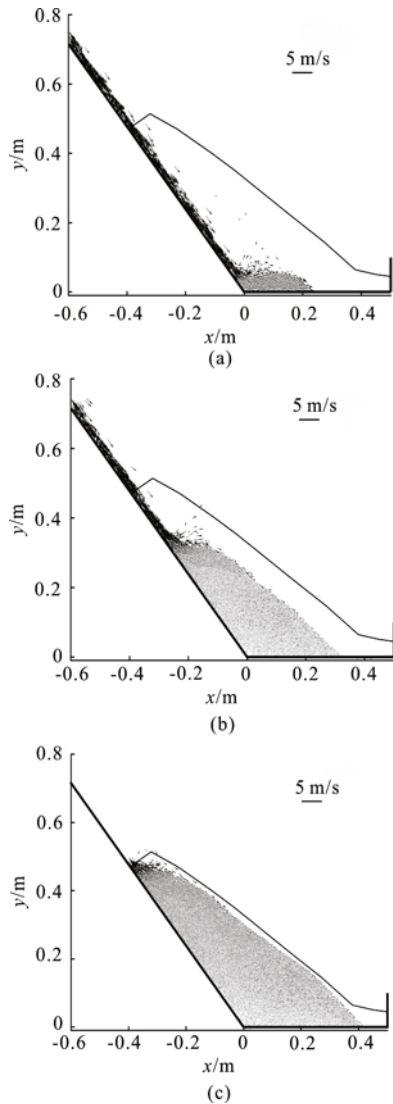


Fig.1 Releasing granular material on a slope, together with the measured deposition profile

For some hillside cities with a high population density, passive mitigation measures may prove to be cost-effective. A series of dry granular experiments^[5] were performed to study the landslide impact on rigid barriers (Fig. 2a). 50 kg of Toyoura sand was used, with a bulk density of 1379 kg/m³. The sand was initially confined in a rectangular box of length 0.5 m and height 0.3 m. It was then released to flow along

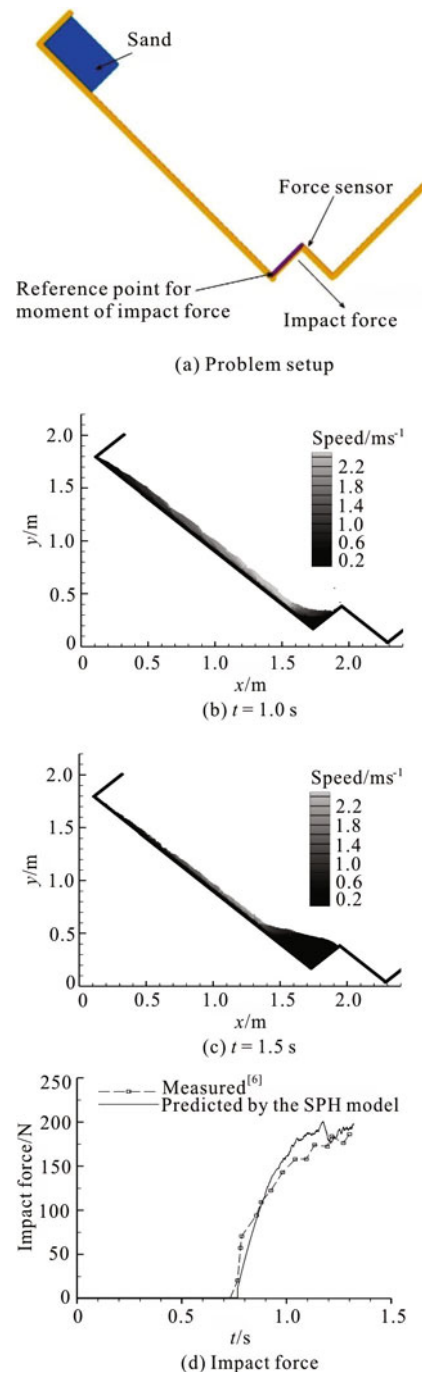


Fig.2 (Color online) Interaction of landslide with a rigid barrier at the toe

the slope and eventually hit a rigid barrier normal to the slope. The distance between the gate and the barrier is 1.8 m, and the height of the barrier is 0.3 m. We consider the case with a slope angle of 45°.

The initial particle spacing is 3.6 mm, resulting in 10 164 particles. ϕ_{crit} is set to 44°. Figures 2(b), 2(c) show the predicted velocity fields at two typical instants. The sand is seen to stretch into a thin layer along the slope and then deposit progressively in front

of the barrier. Later particles impact on the wedge-shaped static zone, which grows with time. Figure 2(d) shows good comparison between measured and predicted forces.

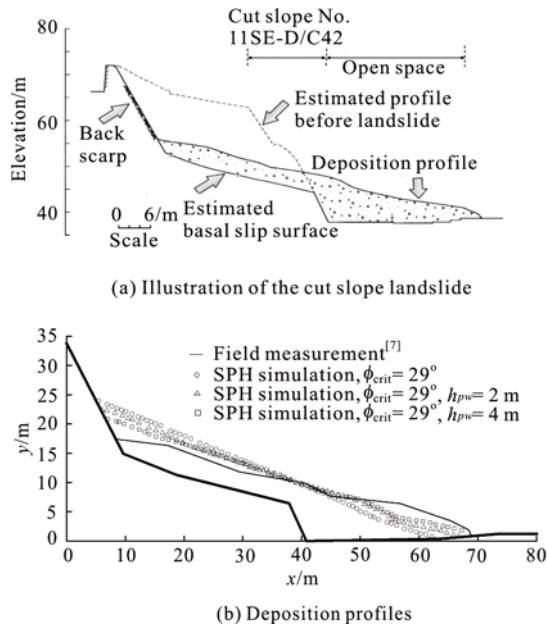


Fig.3 A cut slope landslide near FeiTsu Road, Hong Kong on 13 August, 1995

The final case study considers the FeiTsu cut-slope landslide in Hong Kong. The width of the landslide was 90 m, with a cross-section shown in Fig.3(a). The landslide volume was about 14 000 m³, making it the largest fast-moving cut-slope failure in Hong Kong. The landslide was caused by heavy rain, and the increased groundwater pressure triggered the event. The slope was mainly composed of weathered rock, whose peak strength envelope in terms of effective stress implied an internal friction angle of 35°^[6]. A weak layer was identified at the basal slip surface, consisting of 0.5 m thick kaolinite-rich tuff with low permeability. Laboratory tests showed that the average internal friction angle of this layer was 29° in terms of the effective stress^[6].

In this case, the mobility enhanced by the pore water pressure cannot be ignored. An equivalent friction coefficient is implemented to account for this effect. The pore pressure is denoted by u and the stress tensor can be expressed as $\sigma_{ij} = u\delta_{ij} + \sigma'_{ij}$. Here, σ'_{ij} is the effective stress of the soil which is governed by Eq.(3). Consequently, the equivalent friction coefficient is calculated as

$$\mu_e = \sin \phi_e = \frac{|s_{ij}|}{p} = \frac{|s'_{ij}|}{p' + u} = \frac{\mu_{crit}}{1 + \frac{u}{p'}} \quad (12)$$

Assume an initial layer of water with height h_{pw} flowing uniformly above the basal kaolin layer. The values of u and p' are then estimated as in an infinite landslide model, allowing the equivalent friction angle to be calculated. We further assume that these initial pore pressures remain unchanged as the slide progresses. When h_{pw} is assumed to be 2 m, ϕ_e at the basal slip surface is 23.24°. When increasing h_{pw} to 4 m, this ϕ_e drops to 22.33°. Fig. 3(b) indicates a positive correlation between the water table height and the run-out distance. With an initial water depth of 4 m, the predicted deposition profile agrees well with the field observation. This analysis largely agrees with the static slope stability analysis^[6]. Considering the uncertainties regarding the soil's initial condition and the excess pore pressure variation, it is encouraging that this simple model is capable of giving reasonable predictions.

In summary, a projection method is used to solve the continuum mechanics equations for predicting rapid landslide phenomena in an SPH framework. The normal stress is calculated implicitly via a Poisson equation. It has the advantage over the explicit SPH models by obtaining a smooth stress field without any complicated treatments. Its drawback lies in its inability to consider the soil dilation and the void ratio variation with the normal stress.

References

- [1] Liang D. Evaluating shallow water assumptions in dam-break flows [J]. *Proceedings of the Institution of Civil Engineers-Water Management*, 2010, 163(5): 227-237.
- [2] Liu M. B., Li S. M. On the modeling of viscous incompressible flows with smoothed particle hydrodynamics [J]. *Journal of Hydrodynamics*, 2016, 28(5): 731-745.
- [3] Zhang A. M., Sun P. N., Ming F. R. et al. Smoothed particle hydrodynamics and its applications in fluid-structure interactions [J]. *Journal of Hydrodynamics*, 2017, 29(2): 187-216.
- [4] Pudasaini S. P., Hutter K., Hsiao S. S. et al. Rapid flow of dry granular materials down inclined chutes impinging on rigid walls [J]. *Physics of Fluids*, 2007, 19(5): 053302.
- [5] Moriguchi S., Borja R. I., Yashima A. et al. Estimating the impact force generated by granular flow on a rigid obstruction [J]. *Acta Geotechnica*, 2009, 4(1): 57-71.
- [6] GEO. Report on the FeiTsu road landslide of 13 August 1995 [R]. Hong Kong, China: Geotechnical Engineering Office, 1996, 156.